Catalysis Letters, Vol. 117, Nos. 3–4, September 2007 (© 2007)
DOI: 10.1007/s10562-007-9134-5

Photocatalytic study of polymorphic titania synthesized by ambient condition sol process

Christopher A. Nolph, Daniel E. Sievers, Sujaree Kaewgun, Courtney J. Kucera, Daniel H. McKinney, John P. Rientjes, Jamie L. White, Radhika Bhave, and Burtrand I. Lee*

School of Materials Science and Engineering, Clemson University, Clemson, SC 29634, USA

Nanocrystalline titania of different phases were produced by ambient condition sol process with phase control originating from alterations in experimental variables. The produced titania photocatalysts were characterized by use of x-ray diffraction, BET surface area, transmission electron microscopy and related to methyl orange degradation. The results showed that the photocatalytic activity of brookite and anatase phase titania samples to be greater than that of Degussa P-25 and rutile phase titania sample. In addition, brookite, due to surface area considerations, appears to be the most photocatalytically active phase of titania.

KEY WORDS: titania; phase Comparison; photocatalysis; methyl Orange.

1. Introduction

Titanium(IV) Oxide (titania, TiO_2), well-known to exist as three polymorphs: anatase, rutile, and brookite, has received much attention as a photocatalyst [1–8]. Each phase is known to possess similar band gap energies, approximately 3.2 eV, which lies in the UV region [9]. The irradiation of UV light to any of these phases leads to the creation of electron-hole pairs which follow several pathways of propagation and termination but more importantly can react with water, oxygen or other constituents absorbed on the surface and produce free radicals [1,9]. Degussa Aeroxide TiO_2 P-25 (P-25), 79% anatase 21% rutile and commonly used as a commercial reference, has received claim by Coleman et al. [7] to be the best ratio mix of anatase and rutile to conduct photocatalysis when compared to titania prepared by hydrothermal and magnetic deposition methods.

The general physical properties, i.e. density, melting point, etc, of anatase, rutile and brookite are essentially the same. It has been sought out previously to detect differences between the three polymorphs and one area where a difference is thought to exist is with photocatalytic properties. Comparative studies of anatase and rutile have been conducted indicating anatase as the more photocatalytically active phase under ultraviolet light irradiation [10,11]. Real world applications dictate a greater need for an effective photocatalyst that is capable of receiving activation from visible light and even more so with an immobilized system creating the need for a high surface area and high efficiency photocatalyst [17]. The orthorhombic polymorph of titania, brookite, has received less attention in the past due to difficulties in synthesis to yield a single phase product. However, brookite has received increased attention in recent years as new methods were developed [5,6,12–17] though not all have achieved pure brookite phase titania.

This paper will serve as a lead in to future reports covering the effect of doping and surface treatments on titania nanoparticles and the resulting photocatalytic efficiencies in the ultraviolet and visible light regions. The focus of this paper consists of a study on the three polymorphic phases of titania in conjunction to photocatalytic activity facilitated by methyl orange degradation.

2. Experimental

Three different sets of samples of titania were prepared under near identical conditions with variance applied to the experimental variables in order to alter the phase composition of each set of samples. Each set of samples that were synthesized were compared to a commercial standard and to one another in terms of phase, morphology, particulate size, etc. Each sample was prepared by hydrolyzing titanium tetrachloride ($TiCl_4$ – Reagent grade obtained from Aldrich Chemical, Madison, WI and used as received) in an acidic medium, a high concentration of hydrochloric acid

---

*To whom correspondence should be addressed.
E-mail: burt.lee@ces.clemson.edu

(HCl). A varying ratio of isopropyl alcohol to water was utilized as one variable capable of controlling the phase composition of the samples produced [18]. Table 1 outlines the experimental conditions taken to control the phase of titania and contains a corresponding list of sample ID's to be used throughout the rest of this paper.

A commercial titania product Degussa Aeroxide TiO_2 P-25 (P-25), was obtained directly from Degussa and was utilized as a comparison reference for all characterization procedures which followed.

X-ray crystallography (XDS 2000, Scintag PAD V utilizing CuK_α radiation at 1.5406 Å) was used to determine the phase composition of all prepared and commercial samples of TiO_2. Each sample was run with a step size of 0.020° over a 2θ range of 20° to 80°. Crystallite size of the phases present per sample set were calculated by use of the Scherrer equation (Equation 1) where λ is the aforementioned wavelength of CuK_α x-rays and β is the full-width half-height of the peak of interest: (121) for brookite, (110) for anatase and (101) for rutile [17].

$$t = \frac{0.9 \cdot \lambda}{\beta \cdot \cos(\theta)} \tag{1}$$

Brunauer-Emmett-Teller surface area, pore volume and average pore diameter measurements were conducted on a Micromeritics ASAP 2020 automated system determined by N_2 physisorption at −196°C and 200°C degas condition for 3 h prior to analysis. Transmission electron microscopy (TEM) sample preparation consisted of ensuring a fine powder and dispersing approximately 0.01 g in 4 mL of isopropanol. Dispersions were obtained via additional manual communition of the undispersed powder and ultrasonication for a duration of 90 min of the dispersions. An opaque suspension was obtained and was transferred drop-wise to a copper TEM sample grid and the isopropanol was allowed to evaporate. TEM micrographs were obtained from a Hitachi TEM H7600T with an accelerating voltage of 120.0 kV.

A dark condition reaction setup was built and utilized to test the photocatalytic activity with respect to the degradation of methyl orange (MO) under ultraviolet light. A stock MO aqueous solution of 200 μM concentration was initially prepared and stored in dark conditions within a brown glass bottle. One reaction was performed at a time and repeated for verification of results. The final MO concentration after dilution, via the addition of deionized water, was 20 μM to which 0.2 g of the titania photocatalyst was added. Prior to the initiation of the reaction, the suspension and solution were stirred for 30 min and continuously stirred throughout the reaction. The dispersed state of the particles in the obtained suspension was not directly investigated, but the state of the particles can be conjectured to be agglomerated due to the particle size and high surface tensions. The light source used was a Spectroline black light lamp (Model BIB-150B operating at 365 nm and 182 W) which was suspended 14 inches above the MO solution. A constant sample amount was extracted from the beaker containing the suspension at constant time increments dependent on the previously tested time of completion. The suspension was then separated by

Table 1
Experimental Conditions utilized to produce single phase and mixed phase titania

Sample ID	Predominant Phase Present	Mode of Formation	Temperature (°C)	IPA:Water	HCl concentration (M)	Time (hr)
T-Br	Brookite	ACS	83	2:1	0.3	15
T-An	Anatase	ACS	83	1:0	1.0	15
T-Ru	Rutile	ACS	83	2:1	1.4	15
T-Br200	Brookite	Calcination of Br	200	–	–	2
T-An200	Anatase	Calcination of An	200	–	–	2
T-Ru200	Rutile	Calcination of Ru	200	–	–	2

Table 2
Physical Properties of prepared photocatalysts and commercial reference

Sample ID	Crystalline Size			BET Surface Area (m^2/g)	Pore Volume (cm^3/g)	Average Pore Size (Å)
	Anatase (nm)	Brookite (nm)	Rutile (nm)			
P-25	21	–	40	56	0.24	168
T-Br	–	14	–	163	0.10	25
T-An	10	–	–	266	0.25	37
T-Ru	–	–	9	112	0.09	33
T-Br200	–	18	–	157	0.10	27
T-An200	13	–	–	235	0.25	43
T-Ru200	–	–	10	115	0.10	33

means of vacuum filtration (Whatman Anodisc 47 mm discs with 0.02 μm pores) to remove all traces of titania photocatalyst from the solution to prevent scattering. The reaction was monitored by a UNICAM UV/vis spectrometer (Model: 5625) which returned quantitative spectral results of MO degradation. The retained spectral values were used to calculate the ratio of methyl orange degradation (Equation 2) at a chosen constant wavelength of 490 nm where A_0 is the initial 490 nm absorbance peak intensity, A is the instantaneous 490 nm peak intensity and D is the methyl orange degradation percent value. These absorbance values are directly related to the, more relevant, concentration of methyl orange in solution hence C_0 as the initial concentration and C as the instantaneous concentration.

$$D = \frac{A_0 - A}{A_0} \times 100\% = \frac{C_0 - C}{C_0} \times 100\% \qquad (2)$$

3. Results and Discussion

XRD results are shown in Figure 1(a–b). Figure 1(a) contains the diffractograms obtained from those uncalcined samples and Figure 1(b) the diffractograms from the samples which received calcinations (200°C for 2 h). The phases obtained were confirmed by comparison to accepted standard peaks from JCPDS [19–21]. The predominant phases for each set of samples can be seen in Table 1. Calcination of sample T-Br (T-Br200) did yield the formation of a small portion of rutile in the structure.

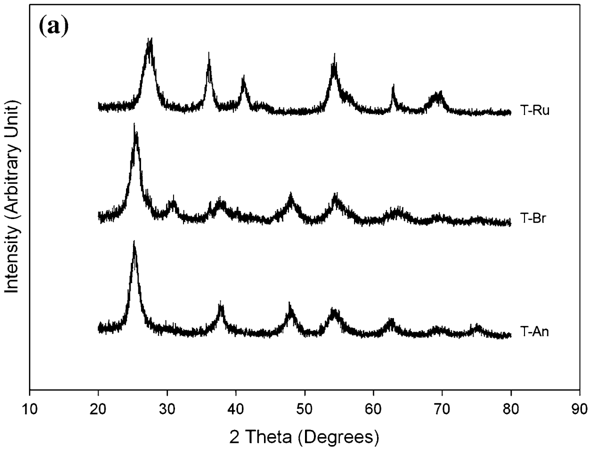

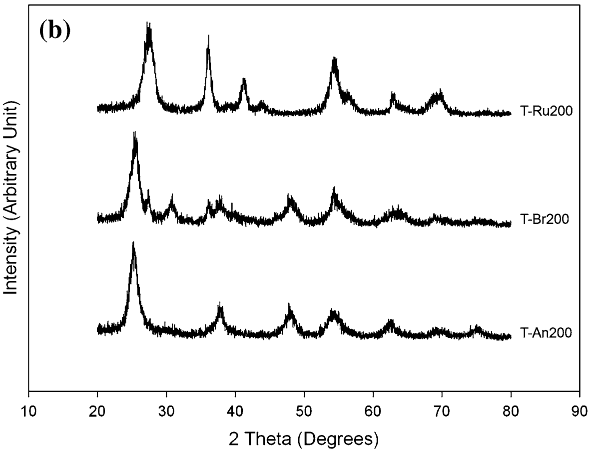

Fig. 1. X-ray diffratograms of (a) as-prepared titania samples and (b) titania samples after 200°C calcination for 2 hours.

An estimation of particle size and particle morphology can be seen in Figure 2(a–c). The particle shape for each phase can be considered identical with little discernable differences. The higher pore volume of T-An200 is apparent in the micrographs as the apparent densities of the particles are lower shown as the faintness of the particles relative to T-Br200 and T-Ru200.

The results of the methyl orange degradation are shown in Figure 3(a–b) where Figure 3(a) is the results of those samples which received no calcinations and Figure 3(b) is the results of those samples which were calcined at 200°C for 2 h. The degradation of the uncalcined samples will not be fully discussed because of the apparent overlap of capabilities in contrast to the clear discernable results obtained for those samples calcined at 200°C for 2 hours. As seen in Figure 3(a) there is little correlation that can be made with respect to phase and photocatalytic activity. This difference that occurs between the uncalcined and calcined samples can be accounted for by the different preparation reaction conditions required to synthesize the different phases. Thus the uncalcined samples have extrinsic differences in their photocatalytic ability. The differences can be accounted for by residual contaminants, namely water, isopropyl alcohol and hydrochloric acid. The results in Figure 3(b), all samples received identical post-synthesis processing, can be seen to show a discernable trend. T-An200, T-Br200 and T-Ru200 all out performed P-25 and T-An200 and T-Br200 were found to possess near identical performance which was greater than that of T-Ru200.

A previous study performed by this group confirmed a correlation between surface area and photocatalytic activity, an inversely proportional relationship with a series of calcined samples considered to be constant phase for the temperature range of interest in this paper [2]. An expected value of degradation can then be interpolated for each sample, T-Br200, T-An200 and T-Ru200, based on their measured surface areas. These predicted values are 88%, 100% and 60% methyl orange degradation after 75 min for T-Br200, T-An200 and T-Ru200 respectively, but the experimental values are 97%, 100% and 80% (these values were obtained by extrapolation of obtained exponential regression functions). This difference in performance can be accounted for by the phase of the respective titania photocatalyst. In addition, despite T-An200 having a higher surface area than T-Br200 (approximately 35%) both phases possess similar photocatalytic activity which signifies

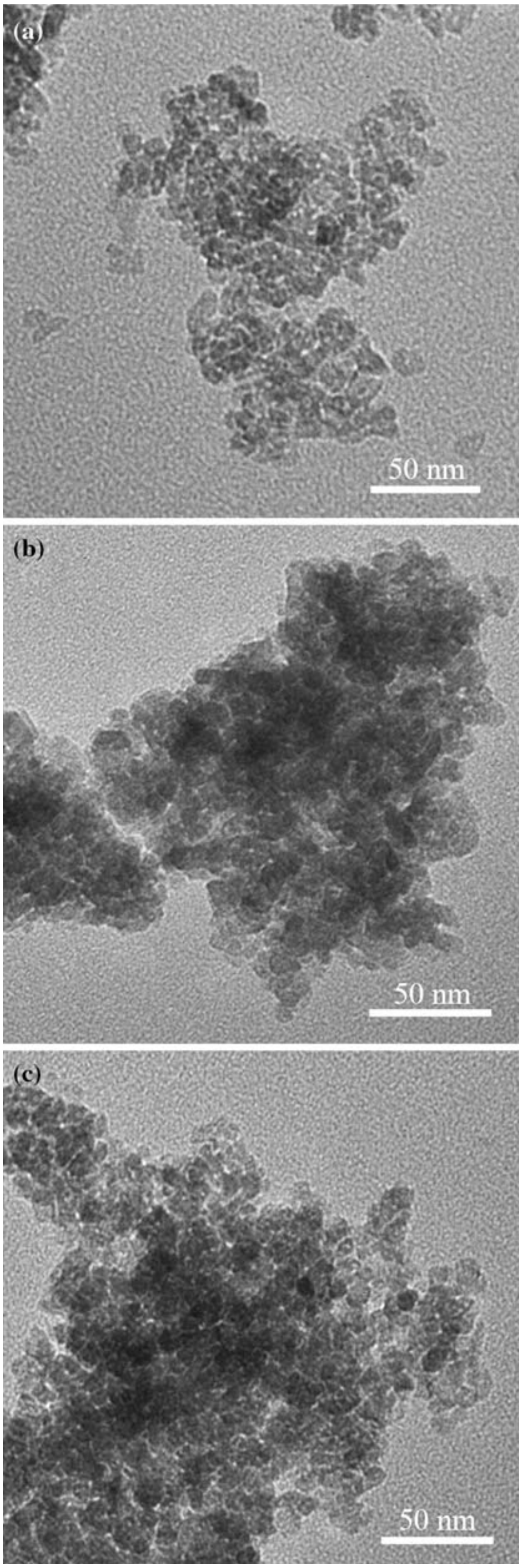

Fig. 2. TEM micrographs of (a) T-An200, (b) T-Br200, and (c) T-Ru200.

brookite as the more photoactive phase, crystallographically, and these claims are receiving an ongoing investigation by this group.

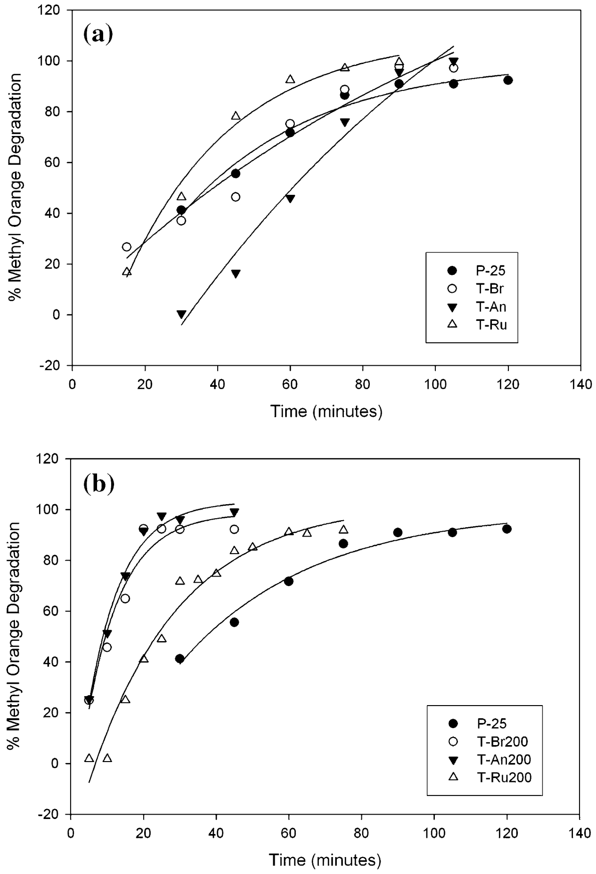

Fig. 3. Methyl orange degradation curves of (a) as-prepared titania samples and (b) titania samples after 200°C calcination for 2 hours both containing P-25 for comparison.

4. Conclusions

Experimentally, the phase composition of titania was successfully controlled using the reaction variables of volumetric ratio of IPA to deionized water and molar concentration of HCl. A dark condition reaction setup was successfully produced and utilized to yield consistent methyl orange degradation results with the aid of the prepared and commercial titania photocatalysts. All samples prepared that were calcined at 200°C out-performed the P-25 samples, and T-Br200 and T-An200 yielded similar photocatalytic activity which was greater than that of T-Ru200. In addition, due to a higher surface area T-An200 and similar activity, T-Br200, brookite, can be stated to have a higher catalytic activity.

Acknowledgment

This research was possible by the Creative Inquiry Undergraduate Program at Clemson University. Partial financial support by Clemson University and the Petroleum Research Fund of American Chemical Society is gratefully acknowledged.

References

[1] A. Fujishima and K. Honda, Nature: London 238 (1972) 37.

[2] R. Bhave, C.A. Nolph, S. Kaewgun and B.I. Lee, Catalysis Comm. (Submitted).

[3] B. Ohtani, J.-I. Handa, S.-I. Nishimoto and T. Kagiya, Chem. Phys. Letters 120 (1985) 292–294.

[4] L.-C. Chen and T.-C. Chou, Ind. Eng. Chem. Res. 32 (1993) 1520–1527.

[5] H. Kominami, Y. Ishii, M. Kohno, S. Konishi, Y. Kera and B. Ohtani, Catalysis Letters 19 (2003) 41–47.

[6] S. Watson, D. Beydoun, J. Scott and R. Amal, J. of Nano. Res. 6 (2004) 193–207.

[7] H.M. Coleman, C.P. Marquis, J.A. Scott, S.-S. Chin and R. Amal, Chem. Eng. Journal 113 (2005) 55–63.

[8] N. Guettai and H.A. Amar, Desalination 185 (2005) 439–448.

[9] A.L. Linsebigler, G. Lu and J.T. Yates Jr., Chem. Rev. 95 (1995) 735–758.

[10] B. Tryba, M. Toyoda, A.W. Morawski, R. Nonaka and M. Inagaki, App. Catalysis B: Env. 71 (2007) 163–198.

[11] M. Andersson, L. Österlund, S. Ljungstörm and A. Palmqvist, J. Phys. Chem. B 106 (2002) 10674–10679.

[12] B.I. Lee, X. Wang, R. Bhave and M. Hu, Mat. Letters 60 (2006) 1179–1183.

[13] H. Kominami, M. Kohno and Y. Kera, J. of Mat. Chem. 10 (2000) 1151–1156.

[14] K.-R. Zhu, M.-S. Zhang, J.-M. Hong and Z. Yin, Mat. Sci. & Eng. A 403 (2005) 87–93.

[15] A. Pottier, C. Chanéac, E. Tronc, L. Mazerolles and J.-P. Jolivet, J. Mat. Chem. 11 (2001) 1116–1121.

[16] Y. Zheng, E. Shi, X. Cui, W. Li and X. Hu, J. of Mat. Sci. Letters 19 (2000) 1445–1448.

[17] L.S. Birks and H. Friedman, J. App. Phys. 17 (1946) 687–692.

[18] R. Bhave and B. I. Lee, J. Mat. Sci. Eng. A. (Accepted).

[19] JCPDS #29–1272.

[20] JCPDS #29–1276.

[21] JCPDS #29–1360.